*4486–4494* *Nucleic Acids Research, 2006, Vol. 34, No. 16* *Published online 31 August 2006*
*doi:10.1093/nar/gkl609*

# Transcriptional and phenotypic comparisons of *Ppara* knockout and siRNA knockdown mice

**Angus T. De Souza*, Xudong Dai, Andrew G. Spencer[1], Tom Reppen[1], Ann Menzie[1], Paula L. Roesch[1], Yudong He, Michelle J. Caguyong, Sherri Bloomer, Hans Herweijer[1], Jon A. Wolff[1], James E. Hagstrom[1], David L. Lewis[1,*], Peter S. Linsley and Roger G. Ulrich**

Rosetta Inpharmatics, a wholly owned subsidiary of Merck & Co. Inc., 401 Terry Avenue North, Seattle, WA 98109, USA and [1]Mirus Bio Corporation, 505 S. Rosa Road, Madison, WI 53719, USA

Received July 21, 2006; Revised August 3, 2006; Accepted August 4, 2006

## ABSTRACT

**RNA interference (RNAi) has great potential as a tool for studying gene function in mammals. However, the specificity and magnitude of the *in vivo* response to RNAi remains to be fully characterized. A molecular and phenotypic comparison of a genetic knockout mouse and the corresponding knockdown version would help clarify the utility of the RNAi approach. Here, we used hydrodynamic delivery of small interfering RNA (siRNA) to knockdown peroxisome proliferator activated receptor alpha (*Ppara*), a gene that is central to the regulation of fatty acid metabolism. We found that *Ppara* knockdown in the liver results in a transcript profile and metabolic phenotype that is comparable to those of *Ppara*$^{-/-}$ mice. Combining the profiles from mice treated with the PPARα agonist fenofibrate, we confirmed the specificity of the RNAi response and identified candidate genes proximal to PPARα regulation. *Ppara* knockdown animals developed hypoglycemia and hypertriglyceridemia, phenotypes observed in *Ppara*$^{-/-}$ mice. In contrast to *Ppara*$^{-/-}$ mice, fasting was not required to uncover these phenotypes. Together, these data validate the utility of the RNAi approach and suggest that siRNA can be used as a complement to classical knockout technology in gene function studies.**

## INTRODUCTION

The use of genetic knockout mice has greatly facilitated the study of gene function in a wide range of biological processes and has aided in the discovery of new therapeutics. Indeed, a retrospective investigation of knockouts of top-selling drug targets revealed a correlation between phenotypes, mechanism of action and therapeutic effectiveness (1). However, there are drawbacks to the use of knockout technology. These include the time required to generate the founder knockout animal and to breed a population of sufficient size for the acquisition of statistically significant data, the difficulties in generating knockout animals for embryonic lethal genes and the fact that knockout technology is practically limited to a few strains of mice and not readily applicable for use in other species.

The discovery that small interfering RNA (siRNA) could be used in mammalian cells to elicit RNA interference (RNAi) has opened another avenue for studying gene function in mammals (2). The use of siRNA could circumvent some limitations of knockout technology, allowing rapid generation of relatively large numbers of knockdown mice of practically any strain of interest. Indeed, there have been several recent reports of the use of RNAi in mice [reviewed in (3)]. However, the paucity of data detailing the molecular and phenotypic effects of delivering siRNA and of the subsequent knockdown of target gene expression in these studies has made it difficult to definitively discern the effectiveness and specificity of the RNAi approach. Here, we performed a molecular and phenotypic comparison of mice treated with siRNA targeting peroxisomal proliferator activated receptor alpha (*Ppara*) and *Ppara* knockout mice.

*Ppara* is a member of the nuclear hormone receptor superfamily and is involved in regulating fatty acid metabolism. In the liver, *Ppara* is expressed exclusively in hepatocytes (4). During an overnight or prolonged fast, fatty acids released from adipose tissue are transported to the liver, robustly inducing PPARα activity (5). Upon binding fatty acid ligand, PPARα stimulates transcription of genes containing PPARα response elements in their enhancers, most notably genes involved in lipid metabolism and energy homeostasis (6). Drugs belonging to the fibrate class act as synthetic PPARα ligands and can be used to treat patients with hypertriglyceridemia. Consistent with the proposed role for PPARα, these drugs improve plasma lipid profiles by promoting fatty acid β-oxidation and reducing hepatic triglyceride production.

*To whom correspondence should be addressed. Tel: +1 608 441 2858; Fax: +1 608 441 2880; Email: dave.lewis@mirusbio.com
*Correspondence may also be addressed to Angus T. De Souza. Tel: +1 425 246 5837; Email: angus_desouza@w-link.net

Analyses of *Ppara*$^{-/-}$ mice have provided valuable insight into the role of PPARα in regulating metabolism. Interestingly, young adult *Ppara*$^{-/-}$ mice have slightly elevated levels of cholesterol but do not display an obvious phenotype under normal dietary conditions (7,8). However, under fasting conditions or when fed a high fat diet, these mice suffer from hypoglycemia and dyslipidemia, and accumulate massive amounts of lipid in their livers (5,7,9). These phenotypes can be partially explained by an inability of the *Ppara*$^{-/-}$ mice to meet energy demands and a rate of fatty acid uptake by the liver that exceeds the capacity of the liver to secrete triacylglycerols. In contrast to young adult *Ppara*$^{-/-}$ mice, aged *Ppara*$^{-/-}$ mice are obese and have increased serum triglycerides in the absence of fasting (10). These phenotypes were found to be sexually dimorphic, being more pronounced in females than in males.

In this study, we used hydrodynamic tail vein injection to deliver siRNA targeting *Ppara* and compared resulting genome-wide transcriptional profiles and phenotypes to those of *Ppara*$^{-/-}$ mice. We found that knockdown of *Ppara* using RNAi results in a transcript profile in the liver that is highly comparable, both in magnitude and direction, to that observed in *Ppara*$^{-/-}$ mice. Phenotypic analyses revealed that siRNA-treated mice displayed hypoglycemia and hypertriglyceridemia, phenotypes observed in similarly aged *Ppara*$^{-/-}$ mice. Together, these results indicate that hydrodynamic delivery of siRNA can be effectively used to study gene function in the liver of mice.

## MATERIALS AND METHODS

### siRNAs

The siRNAs used in this study were obtained from Dharmacon and consisted of 21 nt sense and antisense oligonucleotides each containing fluoro substitutions at the 2′ position of pyrimidine nulceotides, a 5′-$PO_4$ and a two deoxynucleotide overhang at the 3′ end. The 2′ACE protected oligonucleotides were purified by HPLC and then deprotected according to the manufacturer's instructions. Control siRNA targeting the secreted alkaline phosphatase reporter gene (SEAP, GenBank accession no. U89937): sense 5′-pAGGGcAAcuuccAGAccAudTdT-3′, antisense 5′-pAuGGucuGGAAGuuGcccudTdT-3′; *Ppara* (GenBank accession no. NM_011144) siRNA#1: sense 5′-pGAucGGAGcuGcAAGAuucdAdT-3′, antisense 5′-pGGAucuuGcAGcuccGAucdAdT-3′; *Ppara* siRNA#2: sense 5′-pucAcGGAGcucAcAGAAuudCdT-3′, antisense 5′-pAAuucuGuGAGcuccGuGAdCdT-3′; *Ppara* siRNA#3: sense 5′-pGAAGuucAAuGccuuAGAAdAdT-3′, antisense 5′-puucuAAGGcAuuGGAcuucdAdT-3′. Nucleotides containing 2′-fluoro substitutions are lower-case; d, deoxynucleotides; p, 5′ $PO_4$. Sense and antisense oligonucleotides for each target sequence were annealed by mixing equimolar amounts of each and heating to 94°C for 5 min, cooling to 90°C for 3 min, then decreasing the temperature in 0.3°C steps 250 times, holding at each step for 3 s.

### Primary hepatocyte isolation and transfection

Primary hepatocytes were harvested from adult mice (strain C57BL/6) using the two-step collagenase perfusion procedure as described previously (11). Hepatocyte viability was 85–90% as determined by Trypan blue exclusion. Hepatocytes were plated at a density of $1.5 \times 10^5$ cells per well in collagen coated 12-well plates. Cells in triplicate wells were transfected with siRNA at a final concentration of 100 nM using TransIT®-siQuest (Mirus Bio Corporation) according to the manufacturer's protocol, 24 h post plating. Hepatocytes were harvested 24 h after transfection and total RNA was isolated with Tri Reagent (MRC, Inc.).

### Mice and injection procedures

All animal studies were conducted at Mirus Bio Corporation with approval from Mirus' Institutional Animal Care and Use Committee. Six- to eight-week-old mice (strain C57BL/6, 19–21 g) were obtained from Harlan Sprague Dawley Inc. and housed at least 10 days on a 12 h light/dark cycle before injection. Mice had free access to food and water throughout the course of the experiments (Harlan Teklad Rodent Diet). For siRNA delivery, mice were injected in the tail vein using the hydrodynamic technique without anaesthesia as described previously (12). Briefly, siRNA (40 μg) was diluted in a volume of Ringer's solution (147 mM NaCl, 4 mM KCl and 1.13 mM $CaCl_2$) equal to 10% of the animal's body weight. The entire volume was injected into the tail vein in 5–7 s using a 3 ml syringe fitted with a 27 gauge needle.

### Liver harvest and RNA isolation

Mice had free access to food throughout the duration of the experiments and were sacrificed within 1 h of each other. Total RNA was isolated from mouse liver using the RNeasy Midi Kit (Qiagen) according to the manufacturer's protocol with minor modification. Briefly, mouse liver was harvested and immediately placed in 30 ml of RLT buffer and homogenized for 45 s using a PRO200 homogenizer (PRO Scientific). Homogenates were spun at 4000 r.p.m. for 20 min in a RT7 Plus centrifuge (Sorvall). Supernatant (2 ml) was transferred to a new tube and 1 vol of 50% ethanol was added before loading the RNeasy column. The manufacturer's protocol was followed for the rest of the procedure.

### Quantitative PCR Assays

Total RNA (500 ng) was reverse transcribed using SuperScript III (Invitrogen) and oligo-dT primers according to the manufacturer's protocol. Quantification of gene-specific mRNA levels was performed by RT-qPCR using an iCycler iQ system (Bio-Rad). Relative levels of *Ppara* and GAPDH mRNA were measured in biplex reactions performed in triplicate using TaqMan® Universal PCR Master Mix and the TaqMan® Gene Expression Assay for *Ppara* (Applied Biosystems) as per the manufacturer's protocol. The GAPDH primers and probe (IDT) were as follows: GAPDH-forward, 5′-AAATGGTGAAGGTCGGTGTG-3′; GAPDH-reverse, 5′-CATGTAGTTGAGGTCAATGAAGG-3′; and GAPDH-probe, 5′-Hex/CGTGCCGCCTGGAGAAACCTGCC/BHQ-3′.

### Microarray procedures

Expression profiling was carried out using custom arrays consisting of ~23 000 60mer oligonucleotides (plus control sequences) representing mouse genes as described previously (13). All hybridizations were performed in duplicate, with

fluor reversal (Cy3 or Cy5) in the second hybridization. For knockdown mice, each experiment consisted of three groups injected either with *Ppara* siRNA, control siRNA or injection buffer alone (Ringer's). RNAs from individual siRNA-treated animals and buffer-treated animals were hybridized against a pool of RNA from time-matched buffer-treated animals. *Ppara*$^{-/-}$ mice originated from the colony established at the National Cancer Institute (8). For fenofibrate treatment (200 mg/kg/day) wild-type (C57BL/6) and *Ppara*$^{-/-}$ mice (6 animals per group) were treated for 1 and 7 days. RNA from individual animals were paired according to their genetic background and hybridized against a pool of RNA (6 animals) from time-matched wild-type or *Ppara*$^{-/-}$ mice, respectively. The transcriptional response for *Ppara*$^{-/-}$ mice was determined by hybridization of RNA against a wild-type pool.

### Statistical tests

Significance between groups was determined using a two-tailed *t*-test of either unequal [e.g. Experiments A and B, treatments ($n > 15$) versus control siRNA ($n = 4$)] or equal variance [e.g. Experiment C ($n = 4$)]. The significance of Pearson product-moment correlation coefficients ($r$) was determined using *t*-distribution tables for a two-tailed test and the formula:

$$t = (r)\sqrt{\frac{N-2}{1-r^2}} \quad \mathrm{df} = N - 2,$$

where $N$ = number of pairs.

## RESULTS

### Delivery of *Ppara* siRNA to mice by hydrodynamic injection results in knockdown of *Ppara* expression in liver

We first screened five siRNAs against *Ppara* for activity using mouse primary hepatocytes. In anticipation of *in vivo* studies, the siRNAs were synthesized with 2′F substitutions on pyrimidines and 2′-H substitutions in the 2 nt at each 3′ end to increase nuclease resistance. We found that three of the five siRNAs (*Ppara* siRNA#1, #2 and #3) were highly active in this *in vitro* system (Figure 1A).

Our initial studies in mice were composed of two independent experiments, A and B. In both experiments, *Ppara* siRNA#1 (40 μg) was delivered to 6- to 8-week-old C57Bl/6 female mice using hydrodynamic tail vein injection. Control groups included mice injected with a non-targeting siRNA (control siRNA) or Ringer's buffer alone. Livers were harvested 24 h after injection. A pairwise comparison of the *Ppara* siRNA-treated groups to the groups treated with control siRNA revealed a significant ($P \leqslant 0.01$) average reduction in *Ppara* mRNA as determined by quantitative PCR (RT-qPCR) (Figure 1B). The *Ppara* RT-qPCR data across all individuals in our studies correlated significantly ($r = 0.81$, $P < 0.001$) with *Ppara* expression in individuals for which data were obtained from high-density microarrays (Figure 1C). The data indicated that the amount of *Ppara* knockdown was variable between mice, ranging from ~80% knockdown to little or no apparent knockdown. This is likely due to variable siRNA delivery efficiency.

### Genome-wide transcript profiles of *Ppara* siRNA-treated mice and *Ppara*$^{-/-}$ mice are concordant

We utilized high-density microarrays to compare the genome-wide transcriptional response in liver of mice injected with *Ppara* siRNA#1 to that of the well-characterized *Ppara*$^{-/-}$ mouse (8). Knockdown mice from Experiment A were used for these initial analyses. Using the ROAST® correlation tool in the Resolver® v5.0 gene expression data analysis system, we identified 622 genes that correlated ($r > 0.7$, $P < 1 \times 10^{-8}$) with *Ppara* expression levels. The transcriptional response for these 622 genes when projected onto the microarray responses of *Ppara*$^{-/-}$ mice revealed high concordance, both in direction and magnitude, with that observed with *Ppara* siRNA#1-treated animals (Figure 2). Transcriptional concordance was also maintained with larger gene sets (3295 genes) representing lower *Ppara* correlation thresholds ($r > 0.5$, $P < 1 \times 10^{-5}$, data not shown). Accordingly, the majority of mice treated with *Ppara* siRNA#1 grouped with *Ppara*$^{-/-}$ mice. However, three mice, *Ppara* siRNA#1 animals 15, 17 and 19, grouped in the clade containing the mice injected with control siRNA or Ringer's buffer alone (Controls, Figure 2). These mice showed little to no *Ppara* knockdown by RT-qPCR and may represent animals with suboptimal siRNA delivery (Figure 1B). Upon visual inspection, the transcript profiles of these three animals does reveal some resemblance to those within the clade containing the majority of the *Ppara* siRNA#1-treated and the *Ppara*$^{-/-}$ mice. The magnitude of the response in these three mice was very low and is likely to be the reason why these animals group in the clade dominated by the control animals. There were other *Ppara* siRNA#1-treated mice displaying only apparently slight *Ppara* knockdown that did group in the clade containing *Ppara*$^{-/-}$ mice. It is possible that it is the change in *Ppara* levels that is important for perturbing expression of genes modulated by *Ppara* rather than the absolute levels of *Ppara*. If the pre-injection levels of *Ppara* expression in these animals were higher than average, then this change would be reflected in the overall transcriptional response to *Ppara* knockdown as observed here, and not necessarily in the absolute level of *Ppara* expression.

### Identification of proximal transcriptional responses to *Ppara* perturbation

In the following analyses, the transcript profiles of *Ppara* knockdown and *Ppara*$^{-/-}$ mice were compared to those of wild-type mice treated with the PPARα agonist fenofibrate in order to identify candidate genes that are proximal to PPARα regulation as well as to further confirm the specificity of the siRNA response (14). Although PPARα agonism is not the precise opposite of *Ppara* knockdown, we expected that genes proximal to PPARα regulation would be oppositely regulated in the two scenarios. Profiles of knockdown mice from Experiments A and B were included in this analysis as well as mice from a third experiment, Experiment C, in which *Ppara* siRNA#1, #2 or #3 were injected and livers harvested at 24, 48 or 96 h. The use of three different siRNAs targeting *Ppara* in Experiment C would help to ensure the profiles

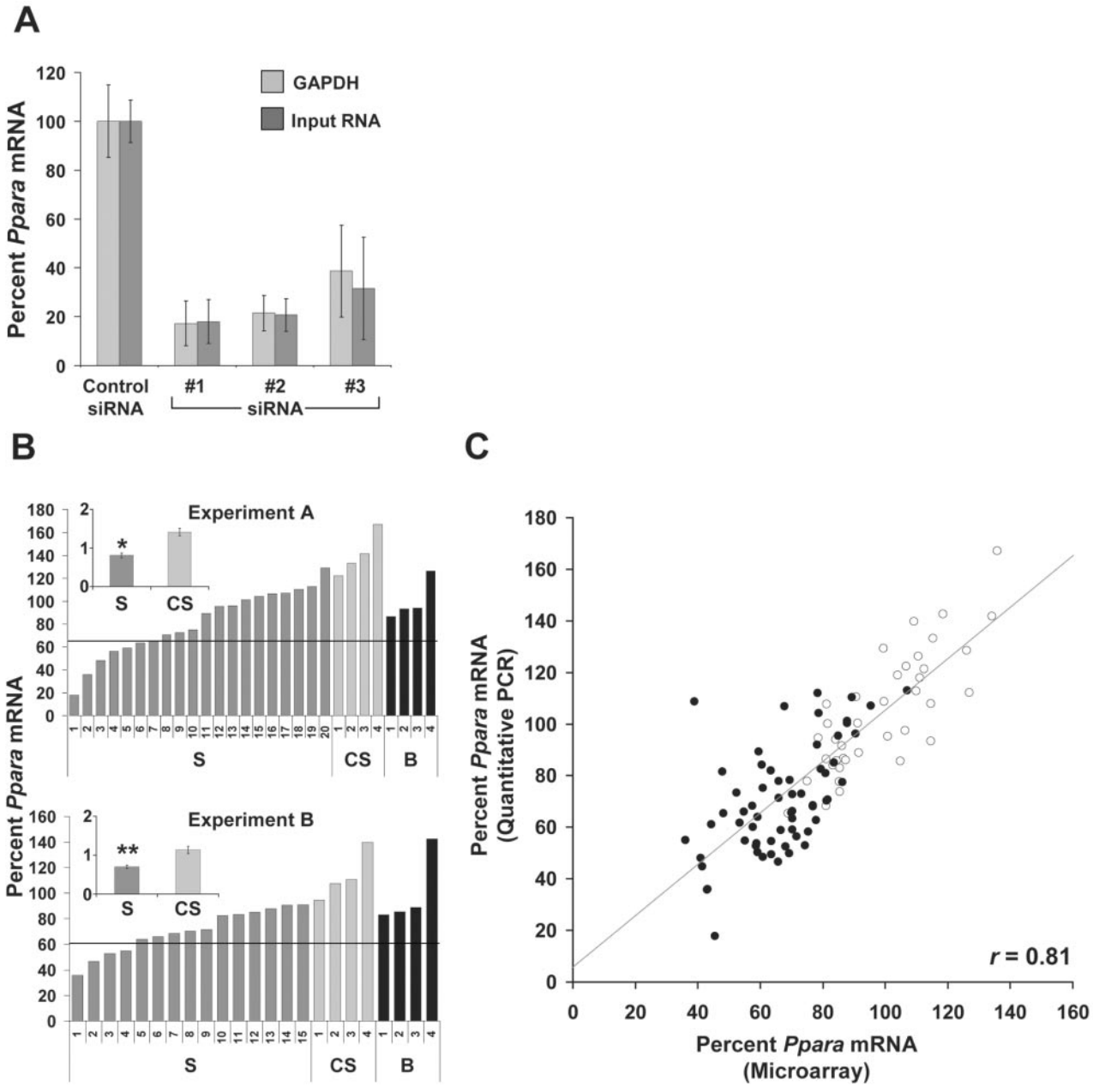


**Figure 1.** *Ppara* knockdown with modified siRNAs *in vitro* and *in vivo*. (**A**) Identification of active *Ppara* siRNAs using transfection of primary mouse hepatocytes. *Ppara* RT-qPCR measurements are normalized to either GAPDH mRNA or input RNA and are expressed relative to the control siRNA group mean. Bars represent the mean (±SD) for $n = 3$. (**B**) *In vivo Ppara* knockdown. *Ppara* RT-qPCR measurements are normalized to GAPDH mRNA and are expressed relative to the buffer group mean. Shown are responses to *Ppara* siRNA#1 treatment at 24 h for individual animals in Experiments A and B. S, *Ppara* siRNA#1; CS, control siRNA; B, injection buffer only. Line indicates 2 SDs below the buffer group mean. Inset, group means (±SEM); *y*-axis is %/100; *, $P < 0.01$; **, $P = 0.01$. (**C**) Regression analysis between microarray and RT-qPCR measurements for *Ppara* mRNA *in vivo*. For microarray measurements, individual animal data is expressed relative to the pool of buffer only treated animals. For RT-qPCR measurements, individual animal data are expressed relative to the appropriate buffer group mean. Shown are the *Ppara* mRNA levels for mice in Experiments A, B and C. Animal 20 (Experiment A) and animals 11–15 (Experiment B) were not profiled and are not represented on the chart. Closed circles, *Ppara* siRNA-treated animals; open circles, buffer and control siRNA-treated animals.

obtained were specific for *Ppara* knockdown and not due to off-target effects of any individual siRNA. A timecourse would allow us to determine the duration of the siRNA effect.

*k*-means clustering was used to separate the 622 genes modulated by *Ppara* siRNA treatment shown in Figure 2 into eight sets (Figure 3A, *x*-axis). Two of the sets, sets 1 and 7, were composed of 71 genes that were oppositely regulated between fenofibrate-treated mice, and *Ppara* siRNA-treated and $Ppara^{-/-}$ mice. When compared to the Gene Ontology (GO) gene sets for Biological Process annotation, these gene sets had significant correlation to metabolic pathways pertaining to oxidative phosphorylation ($P = 1.16 \times 10^{-6}$) and fatty acid β oxidation ($P = 5.50 \times 10^{-3}$), respectively (Table 1). These two pathways have in common the fatty acid metabolic intermediate acetyl-CoA and are known to be directly regulated by PPARα (5). Thus, gene

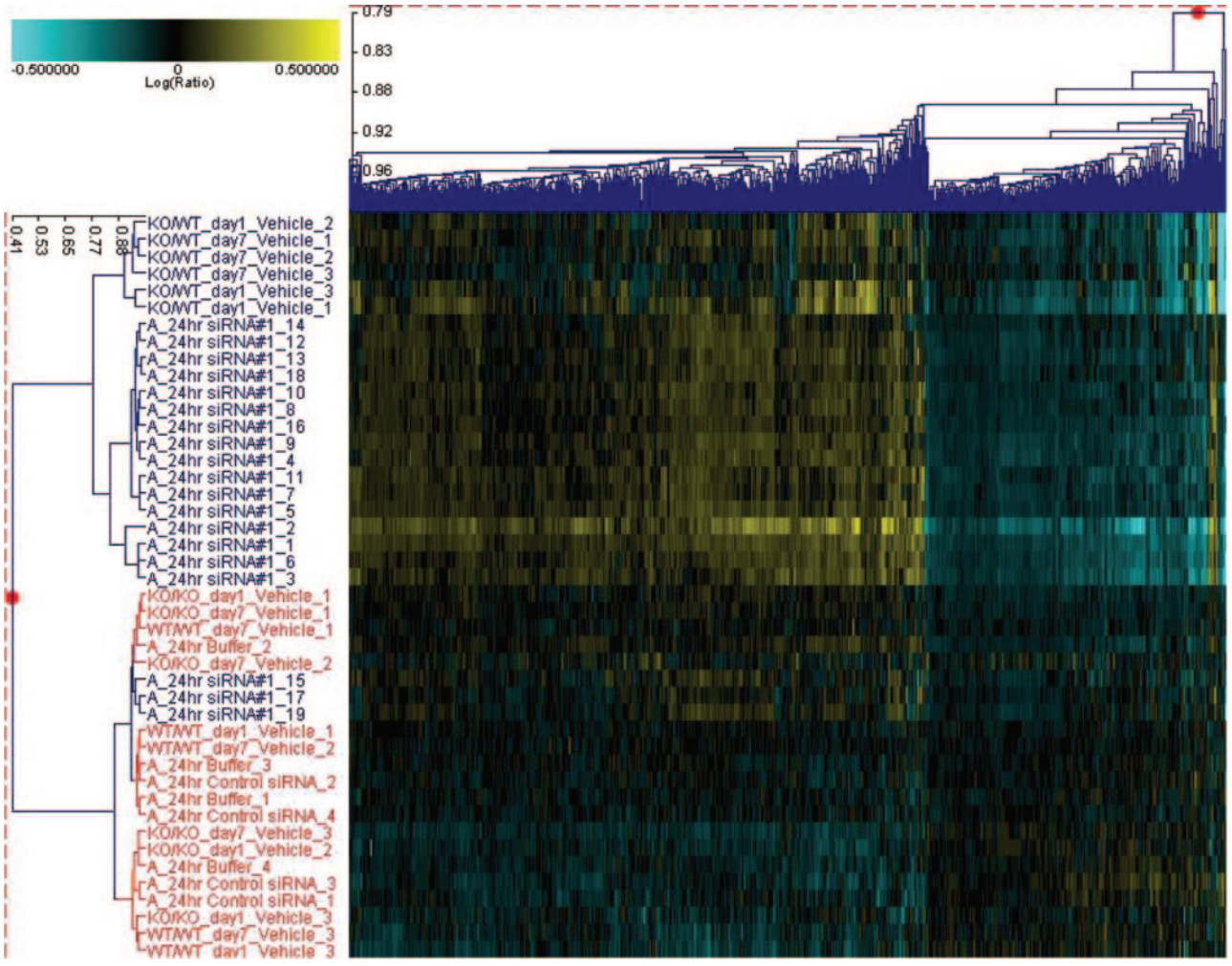


**Figure 2.** Transcriptional concordance between *Ppara* knockdown and *Ppara*$^{-/-}$ animals. Genes correlating to *Ppara* in Experiment A mice were identified by the ROAST® correlation tool in Resolver® v5.0 gene expression data analysis system. Represented is unsupervised agglomerative clustering of 44 experiments (heuristic criteria: Wards minimum variance, similarity measure: Manhattan distance) and 622 genes (heuristic criteria: average link, similarity measure: Euclidean distance). Mice highlighted in blue and red represent treatment and control administrations, respectively.

sets 1 and 7 are likely enriched for genes that are proximal to *Ppara* regulation. In addition, the fact that the genes in sets 1 and 7 show decreased expression in *Ppara* knockdown and *Ppara*$^{-/-}$ mice and increased expression upon fenofibrate treatment is evidence for the on-target effects of the *Ppara* siRNAs used. Two of the remaining gene sets, sets 5 and 8, were also identified to have significant ($P < 0.01$) overlap with other GO gene sets (Table 1). Gene set 8 correlated with components of the ubiquitin-proteosome system and gene set 5 with those involved in mRNA processing. It has been shown that PPARα activity is controlled by regulating stability at the protein level and that *Ppara* mRNA levels are increased during fasting (5,15). Given the important role of PPARα in regulating fatty acid and glucose metabolism, modulation of these systems may be indicative of compensatory mechanisms utilized to maintain metabolic homeostasis when expression or activity of *Ppara* is perturbed. Together, these observations are consistent with the known proximal on-target effects of *Ppara* deficiency (gene sets 1 and 7) and putative distal responses to *Ppara* perturbation (gene sets 2–6 and 8).

Unsupervised agglomerative clustering of all mice using gene sets 1 and 7 resulted in two major experimental clades (Figure 3A, *y*-axis). Clade 1 consists of *Ppara* siRNA#1, #2 and #3-treated mice at 24, 48 and 96 h post administration (with two exceptions) together with the *Ppara*$^{-/-}$ mice. Thus, the signatures of mice treated with three different *Ppara* siRNAs are similar to that of *Ppara*$^{-/-}$ mice, with the effect of the siRNAs persisting to at least 96 h post administration. The fact that a similar signature was obtained using three different *Ppara* siRNAs is evidence that any potential off-target effects of individual siRNAs did not significantly affect the outcome. Clade 2 consists primarily of mice receiving control treatments (highlighted in red). A few *Ppara* siRNA-treated animals are also found in Clade 2. These mice had only a weak signature for genes in sets 1 and 7 used for the cluster analysis, and their presence in Clade 2 likely due to suboptimal siRNA delivery. Conversely, 2 of 56 control mice had signatures of sufficient similarity to *Ppara* knockdown and knockout mice that they were grouped into Clade 1. It is known that *Ppara* expression levels are modulated by dietary intake (5,9). Even though all mice had free access to food for

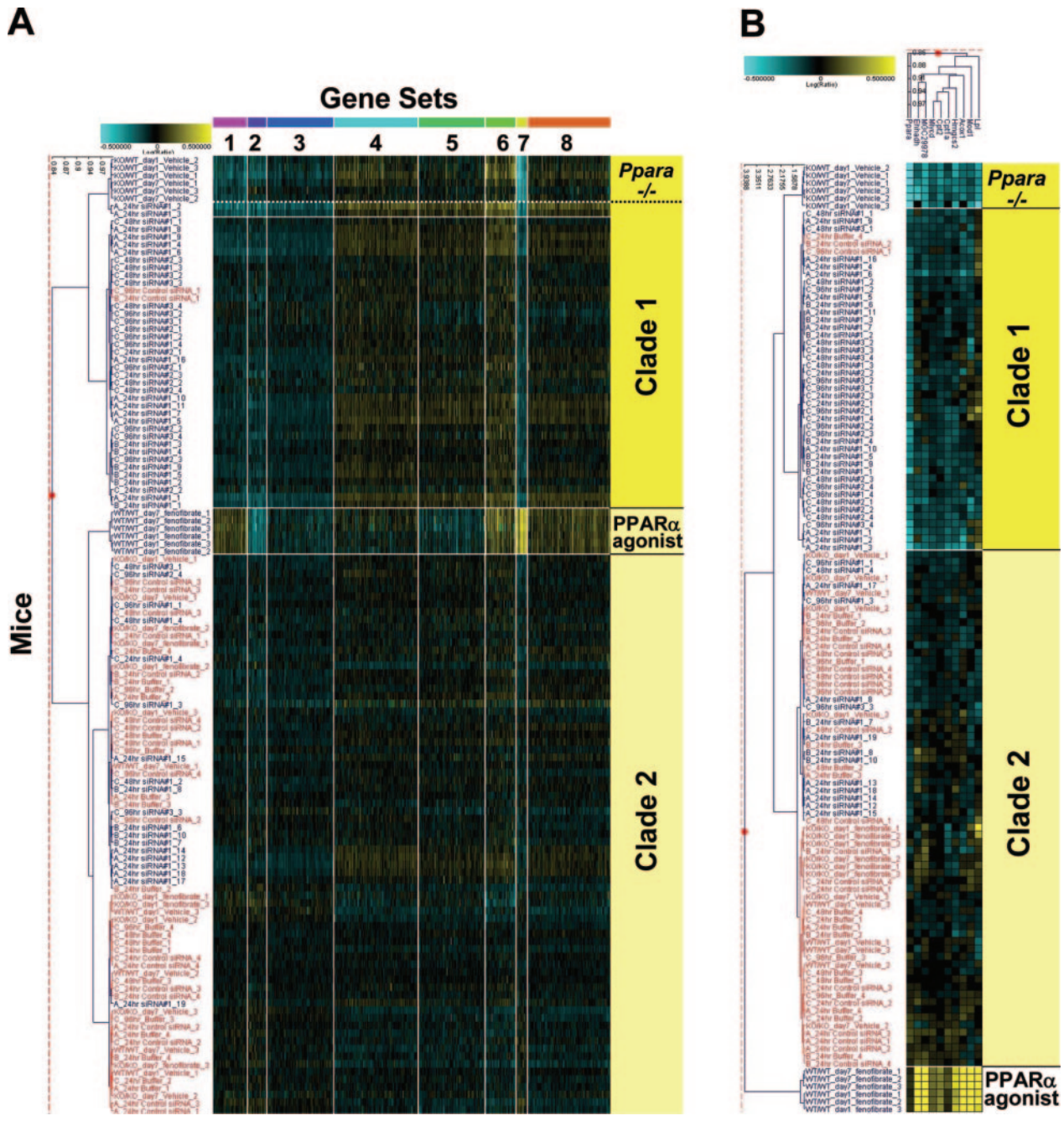


**Figure 3.** On-target responses to *Ppara* perturbation. Mice highlighted in blue and red represent treatment and control administrations, respectively. (**A**) Gene sets 1–8 were identified by *k*-means clustering (similarity measure: Euclidean distance, sorted by deviation) of the 622 genes that have significant transcriptional correlation ($r > 0.7$, $P < 1 \times 10^{-8}$) to *Ppara* across Experiments A and B. Genes in sets 1 and 7 (representing proximal *Ppara* on-target responses, see text) were used for agglomerative clustering (heuristic criteria: Wards minimum variance, similarity measure: maximum distance) of the 125 transcriptional responses illustrated and the results are projected onto all the gene sets identified through *k*-means clustering. Evident are two experimental clades comprised predominantly of mice treated with *Ppara* siRNA #1, #2 and #3 and harvested at 24, 48 and 96 h after injection (Clade 1) and mice treated with buffer only or control siRNA (Clade 2). (**B**) Unsupervised agglomerative clustering of 9 genes (heuristic criteria: Wards minimum variance, similarity measure: Manhattan distance) reported to have functional PPREs in their promoters and under the control of *Ppara*, and the 125 transcriptional responses (heuristic criteria: average link, similarity measure: Euclidean distance). Evident are two experimental clades comprised predominantly of mice treated with *Ppara* siRNA (Clade 1) and mice treated with buffer only or control siRNA (Clade 2).

the duration of the experiments, minor variations in *Ppara* expression due to different feeding behaviours among individual mice were not unexpected. These minor differences appear to be reflected at least to some extent in the transcript profiles of two of the control mice.

We also note that for six of the animals treated with *Ppara* siRNAs in Experiment C a markedly different transcription signature was observed (data not shown). We were unable to reproduce this response in independent experiments, and as the signature was sufficiently high to obscure our analyses

**Table 1.** Gene Ontology Process annotations associated with gene sets 1 to 8

| Set # | Genes | GO Process annotation | *P*-value threshold ($P < 0.01$) | Gene symbol |
|---|---|---|---|---|
| 1 | 53 | energy pathways | 2.12E-07 | 1110020P15Rik, Acads, |
| | | oxidative phosphorylation | 1.16E-06 | Aco2, Atp5d, Atp5g2, Atp5o, |
| | | ATP synthesis coupled electron transport (sensu Eukaryota) | 1.00E-04 | Coasy, Cox7b, Cpt1a, Cpt2, |
| | | ATP synthesis coupled electron transport | 1.00E-04 | Etfb, Ndufs7, Sdhc, Slc25a10, |
| | | electron transport | 1.98E-04 | Uqcr, Uqcrb |
| | | energy derivation by oxidation of organic compounds | 2.96E-03 | |
| | | group transfer coenzyme metabolism | 4.16E-03 | |
| 2 | 31 | | NS | |
| 3 | 105 | | NS | |
| 4 | 132 | | NS | |
| 5 | 104 | mRNA processing | 8.12E-03 | Fip1/1, Fnbp3, Hnrpa3, Rbms2, Rngtt, Sfrs1, Son, Ssb |
| 6 | 49 | | NS | |
| 7 | 18 | fatty acid metabolism | 2.01E-05 | Acadvl, Decr2, Hsd17b4, |
| | | very-long-chain fatty acid metabolism | 2.46E-04 | Peci, Slc25a20 |
| | | peroxisome organization and biogenesis | 6.93E-04 | |
| | | fatty acid beta-oxidation | 5.50E-03 | |
| 8 | 130 | ubiquitin cycle | 2.57E-04 | Fbxl10, Herc2, Hip2, Pja2, |
| | | ubiquitin-dependent protein catabolism | 7.54E-04 | Psmd2, Rnf11, Senp2, Ube1x, |
| | | modification-dependent protein catabolism | 8.48E-04 | Ube2n, Ube2v2, Usp4, Usp47, Usp48 |

NS = not significant.

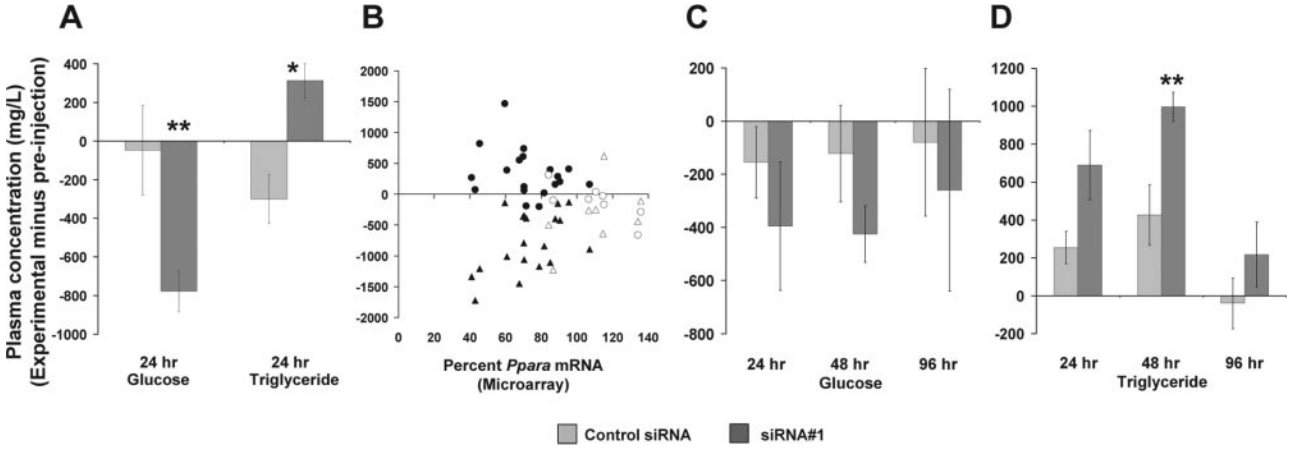


**Figure 4.** Effects of *Ppara* siRNA treatment on plasma concentrations of glucose and triglyceride. (**A**) Glucose and triglyceride group means of mice in Experiment A (±SEM). (**B**) Experiment A individual animal responses for glucose (triangles) and triglyceride (circles) relative to microarray measurements for *Ppara* mRNA (Materials and Methods). Closed symbols, siRNA#1-treated animals; open symbols, control siRNA and buffer-treated animals. (**C** and **D**) Experiment C glucose and triglyceride group means (±SEM), respectively. *$P < 0.01$; **$P < 0.05$. Pre-injection data were subtracted from experimental values to compensate for base-line drift. Female mice were used in Experiment A and male mice in Experiment C.

these mice were excluded. We did not detect evidence of an interferon-like transcriptional response in siRNA-treated animals in any of our experiments, consistent with previous reports using hydrodynamic delivery of naked siRNA (16).

### Treatment with *Ppara* siRNA alters expression of known PPARα targets

As a final test of the specificity of the transcriptional response to *Ppara* knockdown, we identified nine genes present on our microarray and reported in the literature to have functional (i.e. demonstrated by transfection and/or DNA binding assays) peroxisome proliferator response elements (PPREs) in their promoters (17–25). Unsupervised agglomerative clustering of all 125 transcription signatures revealed that genes with functional PPREs were predominantly down-regulated in *Ppara* siRNA-treated animals (Figure 3B, Clade 1). In addition, all nine genes investigated were up-regulated with the PPARα agonist fenofibrate, lending support to this rationale for identifying proximal *Ppara* regulated candidate genes as described in the previous section.

### Mice treated with Ppara siRNA display a similar but distinct phenotype to *Ppara*$^{-/-}$ mice

The phenotype of *Ppara*$^{-/-}$ mice is readily apparent after fasting and includes decreased blood glucose levels and increased triglycerides (5,9,26). To determine the phenotypic effect of *Ppara* knockdown, we collected blood from mice prior to delivery of *Ppara* siRNA#1, and then at 24 h (Experiments A and C), 48 h (Experiment C) and 96 h (Experiment C) after siRNA delivery and performed assays for the appropriate

physiological markers. In these analyses, mice had free access to food and were not purposely fasted before, during or after siRNA delivery.

As expected, we observed an increase in ALT and AST levels in the serum at 24 h due to the effects of the hydrodynamic injection method in the liver. However, these returned to near normal levels by 96 h, and were not significantly different between treated and control groups. In contrast, a group comparison of the *Ppara* siRNA#1-treated animals to those treated with control siRNA in Experiment A revealed a significant decrease in plasma glucose ($P < 0.05$) and increase in triglyceride ($P < 0.01$) concentrations 24 h after siRNA delivery (Figure 4A). *Ppara* knockdown as determined by microarrays relative to all Experiment A animals correlated significantly with modulations in glucose ($r = 0.59$, $P < 0.01$) and triglyceride ($r = -0.60$, $P < 0.001$) concentrations (Figure 4B). The fact that these phenotypes were observed in the absence of fasting is contradictory to the situation in similarly aged *Ppara*$^{-/-}$ mice, where fasting is required. These data indicate that knockdown of *Ppara* expression using siRNA yields a phenotype consistent with the known function of *Ppara*, but one that does not fully recapitulate that of the knockout.

In Experiment C, the treatment related trend for both plasma glucose and triglyceride concentrations was consistent with findings in Experiment A. However, the decrease in blood glucose observed in mice treated with *Ppara* siRNA#1 compared to control mice was not above a statistically significant threshold in Experiment C (Figure 4C), despite the fact that *Ppara* knockdown by siRNA#1 in Experiment C at 24 h was on average equivalent to that observed in Experiment A. The increase in blood triglyceride concentration was statistically significant at 48 h ($P = 0.02$), but increased below a statistically significant threshold at 24 h ($P = 0.20$) and 96 h ($P = 0.41$) (Figure 4D). One possible explanation for the less pronounced phenotype observed in Experiment C versus Experiment A mice may lie in the fact that the Experiment C mice were male, whereas Experiment A mice were female. Sexually dimorphic responses have been reported previously in *Ppara*$^{-/-}$ mice (10,27).

## DISCUSSION

The main objective of this study was to determine if delivery of naked siRNA using hydrodynamic tail vein injection would result in functional inhibition of target gene expression in mouse liver. We chose to target *Ppara*, a well-characterized gene that is critically important in fatty acid metabolism, for which a genetic knockout exists, and whose protein product is the target of therapeutically relevant drugs. We obtained several lines of evidence indicating that delivery of *Ppara* siRNA induced target-specific inhibition. First, quantification of *Ppara* mRNA levels by RT-qPCR or microarrays indicated a significant reduction in mice receiving *Ppara* siRNA compared to those receiving a control. Second, we observed high-transcriptional concordance in both magnitude and direction between *Ppara* siRNA-treated mice and in *Ppara*$^{-/-}$ mice using genome-wide transcriptional profiling. The transcriptional changes were maintained for at least 96 h and were evident with three different siRNAs. Third, sets of genes were identified that were oppositely regulated in siRNA-treated mice compared to mice treated with the PPARα agonist fenofibrate. These gene sets were highly correlated with GO gene sets pertaining to oxidative phosphorylation and fatty acid β oxidation, processes shown previously to be directly regulated by PPARα (5). Fourth, genes known to contain functional PPARα-binding sites in their enhancers were expressed at lower levels in mice receiving *Ppara* siRNA than in control mice. Finally, mice treated with *Ppara* siRNA displayed phenotypes similar to those observed in *Ppara*$^{-/-}$ mice, namely hypoglycemia and hypertriglyceridemia. Thus, both molecular and phenotypic data indicate that functional delivery of naked siRNA to the liver was achieved.

Although the phenotypes of animals treated with *Ppara* siRNA were similar to those reported for *Ppara*$^{-/-}$ mice, we also noted important differences. The most significant difference was the appearance of hypoglycemia and hypertriglyceridemia in *Ppara* siRNA-treated animals in the absence of fasting. This suggests that *Ppara* functions to maintain lipid and glucose homeostasis regardless of the fed state of the animal. This was an unexpected finding given the requirement for fasting to uncover the phenotypes in *Ppara*$^{-/-}$ mice. It is possible that in *Ppara*$^{-/-}$ mice, which are devoid of *Ppara* function throughout development, compensatory mechanisms are induced during growth and development that are sufficient to maintain homeostasis in the fed state, but insufficient in the fasted state. Fasting places a greater reliance on fatty acid oxidation in the liver, which is required to generate ketone bodies needed to supply the energy needs of tissues such as muscle and brain (28). In animals treated with *Ppara* siRNA, we speculate that *Ppara* expression is inhibited before the putative compensatory mechanisms can be fully induced. Alternatively, it is possible that the lack of complete knockdown impacted the phenotypes we observed in the knockdown mice versus those of the *Ppara*$^{-/-}$ mice. We cannot differentiate these possibilities based on the data presented in this report.

How an animal responds to decreased *Ppara* function may also depend on its gender. In our study, we observed more dramatic phenotypes in female *versus* male mice treated with siRNA. Gender-related differences in the phenotypes of *Ppara*$^{-/-}$ mice have also been noted. Djouadi *et al*. (27) found that inhibition of fatty acid oxidation in *Ppara*$^{-/-}$ mice by administration of an irreversible inhibitor of carnitine palmitoyltransferase I resulted in more severe phenotypes in males than in females. These phenotypes could be rescued by pre-treatment with estradiol. In aged *Ppara*$^{-/-}$ mice, Costet *et al*. (10) reported sexually dimorphic phenotypes including obesity and increased serum triglyceride levels in females, and steatosis and increased hepatic triglyceride levels in males. Together, these studies and the present one indicate that the gender of the animal affects how it responds to perturbations in *Ppara* expression.

We have shown here that a single hydrodynamic tail vein injection of a relatively small dose of naked siRNA leads to inhibition of *Ppara* expression in mouse liver to biological effect. These results suggest that this method can be used as a means to uncover gene function *in vivo*. However, there are caveats to the use of siRNA including the potential of off-target effects, incomplete knockdown and non-targeting

of splice variants by the selected siRNA sequence. The use of multiple siRNAs aids in determining if the observed results are due to inactivation of the target gene itself and not due to other effects. Incomplete knockdown of target gene function as well as the transient nature of knockdown using siRNA may also impact the severity and specifics of the phenotype observed. The use of traditional gene knockout technology would be preferable to gene knockdown technology in this sense. However, the cost and time required to generate knockout mice is substantial. In light of this, one potential application of the siRNA approach would be as a screening method to gain insight on the phenotypes of large numbers of genes quickly. The function of the genes identified in the RNAi screen could then be verified or analyzed in more detail by creating knockout strains. The data presented in this report indicate that this could be a viable strategy for gaining an understanding of gene function in liver.

## ACKNOWLEDGEMENTS

We are grateful to Tracy Brunner, Brett Hermanson, Mark Noble, Chris Wooddell, Atsuko Trieloff, Pek Lum, Kenny Wong and the Gene Expression Laboratory for their contributions. Funding to pay the Open Access publication charges for this article was provided by Merck & Co. Inc.

*Conflict of interest statement*. None declared.

## REFERENCES

1. Zambrowicz,B.P. and Sands,A.T. (2003) Knockouts model the 100 best-selling drugs—will they model the next 100? *Nature Rev. Drug Discov.*, **2**, 38–51.
2. Elbashir,S.M., Harborth,J., Lendeckel,W., Yalcin,A., Weber,K. and Tuschl,T. (2001) Duplexes of 21-nucleotide RNAs mediate RNA interference in cultured mammalian cells. *Nature*, **411**, 494–498.
3. Dykxhoorn,D.M., Palliser,D. and Lieberman,J. (2006) The silent treatment: siRNAs as small molecule drugs. *Gene Ther.*, **13**, 541–552.
4. Peters,J.M., Rusyn,I., Rose,M.L., Gonzalez,F.J. and Thurman,R.G. (2000) Peroxisome proliferator-activated receptor alpha is restricted to hepatic parenchymal cells, not Kupffer cells: implications for the mechanism of action of peroxisome proliferators in hepatocarcinogenesis. *Carcinogenesis*, **21**, 823–826.
5. Kersten,S., Seydoux,J., Peters,J.M., Gonzalez,F.J., Desvergne,B. and Wahli,W. (1999) Peroxisome proliferator-activated receptor alpha mediates the adaptive response to fasting. *J. Clin. Invest.*, **103**, 1489–1498.
6. Schoonjans,K., Staels,B. and Auwerx,J. (1996) Role of the peroxisome proliferator-activated receptor (PPAR) in mediating the effects of fibrates and fatty acids on gene expression. *J. Lipid Res.*, **37**, 907–925.
7. Peters,J.M., Hennuyer,N., Staels,B., Fruchart,J.C., Fievet,C., Gonzalez,F.J. and Auwerx,J. (1997) Alterations in lipoprotein metabolism in peroxisome proliferator-activated receptor alpha-deficient mice. *J. Biol. Chem.*, **272**, 27307–27312.
8. Lee,S.S., Pineau,T., Drago,J., Lee,E.J., Owens,J.W., Kroetz,D.L., Fernandez-Salguero,P.M., Westphal,H. and Gonzalez,F.J. (1995) Targeted disruption of the alpha isoform of the peroxisome proliferator-activated receptor gene in mice results in abolishment of the pleiotropic effects of peroxisome proliferators. *Mol. Cell. Biol.*, **15**, 3012–3022.
9. Leone,T.C., Weinheimer,C.J. and Kelly,D.P. (1999) A critical role for the peroxisome proliferator-activated receptor alpha (PPARalpha) in the cellular fasting response: the PPARalpha-null mouse as a model of fatty acid oxidation disorders. *Proc. Natl Acad. Sci. USA*, **96**, 7473–7478.
10. Costet,P., Legendre,C., More,J., Edgar,A., Galtier,P. and Pineau,T. (1998) Peroxisome proliferator-activated receptor alpha-isoform deficiency leads to progressive dyslipidemia with sexually dimorphic obesity and steatosis. *J. Biol. Chem.*, **273**, 29577–29585.
11. Klaunig,J.E., Goldblatt,P.J., Hinton,D.E., Lipsky,M.M., Chacko,J. and Trump,B.F. (1981) Mouse liver cell culture. I. Hepatocyte isolation. *In Vitro*, **17**, 913–925.
12. Lewis,D.L. and Wolff,J.A. (2005) Delivery of siRNA and siRNA expression constructs to adult mammals by hydrodynamic intravascular injection. *Methods Enzymol.*, **392**, 336–350.
13. Hughes,T.R., Mao,M., Jones,A.R., Burchard,J., Marton,M.J., Shannon,K.W., Lefkowitz,S.M., Ziman,M., Schelter,J.M., Meyer,M.R. *et al.* (2001) Expression profiling using microarrays fabricated by an ink-jet oligonucleotide synthesizer. *Nat. Biotechnol.*, **19**, 342–347.
14. Gebel,T., Arand,M. and Oesch,F. (1992) Induction of the peroxisome proliferator activated receptor by fenofibrate in rat liver. *FEBS Lett.*, **309**, 37–40.
15. Blanquart,C., Mansouri,R., Fruchart,J.C., Staels,B. and Glineur,C. (2004) Different ways to regulate the PPARalpha stability. *Biochem. Biophys. Res. Commun.*, **319**, 663–670.
16. Heidel,J.D., Hu,S., Liu,X.F., Triche,T.J. and Davis,M.E. (2004) Lack of interferon response in animals to naked siRNAs. *Nat. Biotechnol.*, **22**, 1579–1582.
17. Bardot,O., Aldridge,T.C., Latruffe,N. and Green,S. (1993) PPAR-RXR heterodimer activates a peroxisome proliferator response element upstream of the bifunctional enzyme gene. *Biochem. Biophys. Res. Commun.*, **192**, 37–45.
18. Barrero,M.J., Camarero,N., Marrero,P.F. and Haro,D. (2003) Control of human carnitine palmitoyltransferase II gene transcription by peroxisome proliferator-activated receptor through a partially conserved peroxisome proliferator-responsive element. *Biochem. J.*, **369**, 721–729.
19. Brandt,J.M., Djouadi,F. and Kelly,D.P. (1998) Fatty acids activate transcription of the muscle carnitine palmitoyltransferase I gene in cardiac myocytes via the peroxisome proliferator-activated receptor alpha. *J. Biol. Chem.*, **273**, 23786–23792.
20. Castelein,H., Gulick,T., Declercq,P.E., Mannaerts,G.P., Moore,D.D. and Baes,M.I. (1994) The peroxisome proliferator activated receptor regulates malic enzyme gene expression. *J. Biol. Chem.*, **269**, 26754–26758.
21. Lee,G.Y., Kim,N.H., Zhao,Z.S., Cha,B.S. and Kim,Y.S. (2004) Peroxisomal-proliferator-activated receptor alpha activates transcription of the rat hepatic malonyl-CoA decarboxylase gene: a key regulation of malonyl-CoA level. *Biochem. J.*, **378**, 983–990.
22. Nicolas-Frances,V., Dasari,V.K., Abruzzi,E., Osumi,T. and Latruffe,N. (2000) The peroxisome proliferator response element (PPRE) present at positions −681/−669 in the rat liver 3-ketoacyl-CoA thiolase B gene functionally interacts differently with PPARalpha and HNF-4. *Biochem. Biophys. Res. Commun.*, **269**, 347–351.
23. Ortiz,J.A., Mallolas,J., Nicot,C., Bofarull,J., Rodriguez,J.C., Hegardt,F.G., Haro,D. and Marrero,P.F. (1999) Isolation of pig mitochondrial 3-hydroxy-3-methylglutaryl-CoA synthase gene promoter: characterization of a peroxisome proliferator-responsive element. *Biochem. J.*, **337**, 329–335.
24. Schoonjans,K., Peinado-Onsurbe,J., Lefebvre,A.M., Heyman,R.A., Briggs,M., Deeb,S., Staels,B. and Auwerx,J. (1996) PPARalpha and PPARgamma activators direct a distinct tissue-specific transcriptional response via a PPRE in the lipoprotein lipase gene. *EMBO J.*, **15**, 5336–5348.
25. Tugwood,J.D., Issemann,I., Anderson,R.G., Bundell,K.R., McPheat,W.L. and Green,S. (1992) The mouse peroxisome proliferator activated receptor recognizes a response element in the 5′ flanking sequence of the rat acyl CoA oxidase gene. *EMBO J.*, **11**, 433–439.
26. Guerre-Millo,M., Rouault,C., Poulain,P., Andre,J., Poitout,V., Peters,J.M., Gonzalez,F.J., Fruchart,J.C., Reach,G. and Staels,B. (2001) PPAR-alpha-null mice are protected from high-fat diet-induced insulin resistance. *Diabetes*, **50**, 2809–2814.
27. Djouadi,F., Weinheimer,C.J., Saffitz,J.E., Pitchford,C., Bastin,J., Gonzalez,F.J. and Kelly,D.P. (1998) A gender-related defect in lipid metabolism and glucose homeostasis in peroxisome proliferator-activated receptor alpha- deficient mice. *J. Clin. Invest.*, **102**, 1083–1091.
28. Eaton,S., Bartlett,K. and Pourfarzam,M. (1996) Mammalian mitochondrial beta-oxidation. *Biochem. J.*, **320**, 345–357.